



Full paper/Mémoire

Pd-poly(N-vinyl-2-pyrrolidone)/KIT-6 nanocomposite: Preparation, structural study, and catalytic activity

Roozbeh Javad Kalbasi^{a,*,b}, Neda Mosaddegh^{a,b}^a Department of Chemistry, Shahreza Branch, Islamic Azad University, 311-86145 Shahreza, Isfahan, Iran^b Razi Chemistry Research Center, Shahreza Branch, Islamic Azad University, Shahreza, Isfahan, Iran

ARTICLE INFO

Article history:

Received 27 April 2012

Accepted after revision 21 June 2012

Available online 11 August 2012

Keywords:

Poly(N-vinyl-2-pyrrolidone)

KIT-6

Polymer-inorganic hybrid material

Pd nanoparticles

Heck reaction

ABSTRACT

The Pd-poly(N-vinyl-2-pyrrolidone)/KIT-6 nanocomposite was prepared by an in situ polymerization method and used as an efficient heterogeneous catalyst for C–C bond formation through the Heck coupling reaction of aryl iodides, bromides and chlorides with styrene. The physical and chemical properties of the catalyst were characterized by XRD, BET, FT-IR, TGA, UV-Vis and TEM techniques. The reactions were performed in methanol-water as solvent and the products were obtained in high yield and purity after a simple work-up. The stability of the nanocomposite catalyst was excellent and could be reused 8 times without much loss of activity in the Heck coupling reaction.

© 2012 Académie des sciences. Published by Elsevier Masson SAS. All rights reserved.

1. Introduction

Palladium-catalyzed cross-coupling reactions are a versatile tool for the generation of C–C bonds [1–5]. Among different methods, the reaction of aryl halides with olefinic compounds, the Heck reaction, is an excellent method for the synthesis of organic compounds [6,7]. Many Pd complexes have been used as homogeneous catalysts in these reactions [8–11]. Although some of the Pd complexes have potential for recycling [11,12], most of them have problems such as deactivation and difficult separation from solution due to the aggregation of Pd nanoparticles formed in situ during the reaction. Thus, it is necessary to develop heterogeneous catalysts which can easily be recovered from the reaction system and reused [13,14].

In catalytic applications, a uniform dispersion of nanoparticles and an effective control of particle size are usually expected. However, nanoparticles frequently aggregate to yield bulk-like materials, which greatly

reduce the catalytic activity and selectivity. Therefore, they must be embedded in a matrix such as polymer or macromolecular organic ligands [15,16]. However, nanoparticle-polymer composites usually suffer from disadvantages such as the absence of complete heterogeneity and high temperature annealing, which generally cause thermal degradation of organic polymers. In addition, to avoid the problems associated with metal nanoparticles such as homogeneity, recyclability and the separation of the catalyst from the reaction system, some other works have focused on immobilizing metal nanoparticles on suitable support materials such as in the pores of heterogeneous supports like ordered mesoporous silica [17,18]. Although nanoparticle-mesoporous materials are completely heterogeneous, the hydrophilicity of these catalysts causes a reduction in their activity in organic reactions. Therefore, preparation of organic-inorganic hybrid catalysts with a hydrophobe-hydrophile nature is interesting.

In the last decade, mesoporous materials with two-dimensional (2D) hexagonal (*p6mm*) structures have been discovered such as MCM-41 and SBA-15 [19–22]. Recently, Ryoo and co-workers [23] reported a new cubic mesoporous silica material named KIT-6, which was prepared using

* Corresponding author.

E-mail addresses: rkalbasi@iaush.ac.ir, rkalbasi@gmail.com (R.J. Kalbasi).

triblock copolymer EO₂₀PO₇₀EO₂₀ (P123) as the mesopore-directing agent and n-butanol as additive under acidic conditions. KIT-6 exhibits a three-dimensional (3D) cubic *la3d* symmetric structure with an interpenetrating bicontinuous network of channels [24]. KIT-6 possesses large readily tunable pores with thick pore walls, high hydrothermal stability, high specific surface area and large pore volume. KIT-6 and materials so on are expected to be superior to mesoporous structures with one or two-dimensional channels due to better dispersion of catalyst and faster diffusion of reactants and products during reaction in the 3D interconnected mesoporous material [25–27]. However, like other siliceous mesoporous materials, the facile functionalization of KIT-6 is essential for the potential application as catalyst.

Hybrid organic–inorganic polymers have received increasing interest from research groups because of their unique properties [28–31]. Nevertheless, among the different researches on these materials, there are relatively a few reports on the application of an organic–inorganic hybrid polymer as a heterogeneous catalyst [32–35]. Recently, in our previous studies [36–39], hybrid organic–inorganic polymers were used as catalysts.

These organic–inorganic hybrid materials could be prepared by various methods, depending on what kind of interaction is employed between organic polymers and inorganic elements, or on how organic moieties are introduced to inorganic phases [40]. In most cases, incorporation of polymer species into mesoporous silica and other inorganic materials are performed with the organosilica precursors. However, the bridged organosilanes precursors either involve complicated synthesis and purification method or are very expensive. Therefore, preparation of organic–inorganic hybrid polymers without using bridged organosilanes precursors is highly desirable. An in situ polymerization, which is the simultaneous polymerization of organic monomers in the presence of mesoporous materials, is an important and inexpensive method for the preparation of composite materials without chemical interaction.

In continuing our previous works to develop new polymer–inorganic hybrid materials based on SBA-15 with 2D hexagonal (*p6mm*) structures as heterogeneous catalysts [36–39], herein, we will introduce a novel and efficient heterogeneous polymer hybrid catalyst based on KIT-6 with 3D cubic *la3d* symmetric structure, for Heck reaction. The catalyst showed good activity besides excellent reusability in the Heck reaction.

2. Materials and methods

2.1. Chemicals supply

All chemicals were obtained from Sigma–Aldrich, Merck and were used without further purification.

2.2. Instruments and characterization

The samples were analyzed using FT-IR spectroscopy (using a Perkin Elmer 65 in KBr matrix in the range of 4000–400 cm^{−1}). The BET specific surface areas and BJH

pore size distribution of the samples were determined by adsorption–desorption of nitrogen at liquid nitrogen temperature, using a Series BEL SORP 18. The X-ray powder diffraction (XRD) of the catalyst was carried out on a Bruker D8Advance X-ray diffractometer using nickel filtered Cu K α radiation at 40 kV and 20 mA. The thermal gravimetric analysis (TGA) data were obtained by a Setaram Labsys TG (STA) in a temperature range of 30–650 °C and heating rate of 10 °C/min in N₂ atmosphere. Transmission electron microscope (TEM) observations were performed on a JEOL JEM.2011 electron microscope at an accelerating voltage of 200 kV using EX24093JGT detector in order to obtain information on the size of Pd nanoparticles and the DRS UV-Vis spectra were recorded with JASCO spectrometer, V-670 from 190 to 2700 nm.

2.3. Catalyst preparation

2.3.1. Preparation of KIT-6

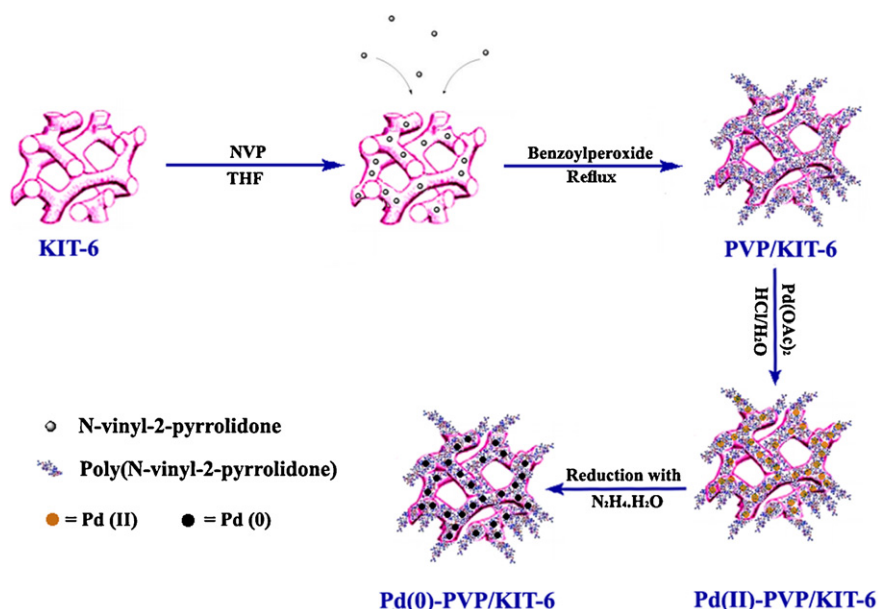
The large pore 3D (*la3d*) cubic mesostructure, designated as KIT-6, was prepared using a Pluronic P123 (EO₂₀PO₇₀EO₂₀) template as a structure directing agent and tetraethylorthosilicate (TEOS) as the silica precursor. In a typical synthesis, 6 g (1.034 mmol) of P123 and 6 g (81 mmol) of n-butanol were dissolved in 270 g (15 mol) of distilled water and 11.4 g (0.115 mol) of concentrated hydrochloric acid (37 wt.% HCl). To this mixture, 12.9 g (0.061 mol) of TEOS was added. The mixture was stirred at 45 °C for 24 h for the formation of the mesostructured product. Subsequently, the reaction mixture was heated for 24 h at 95 °C under static conditions for hydrothermal treatment. The solid product was then filtered, washed with deionized water and dried at 100 °C. Finally, the samples were calcined at 550 °C for 6 h to remove the template.

2.3.2. Preparation of Poly(*N*-vinyl-2-pyrrolidone)/KIT-6 (PVP/KIT-6)

N-vinyl-2-pyrrolidone (NVP) (0.5 mL, 4.6 mmol) and KIT-6 (0.5 g) in 7 mL tetrahydrofuran (THF) were placed in a round bottom flask. Benzoyl peroxide (3% mol, 0.034 g) was added and the mixture was heated to 65–70 °C for 5 h while being stirred under N₂ gas. The resulting white fine powder composite (PVP/KIT-6) was collected by filtration, washed several times with THF, and finally dried at 60 °C under reduced pressure.

2.3.3. Preparation of Pd nanoparticle-poly(*N*-vinyl-2-pyrrolidone)/KIT-6 (Pd-PVP/KIT-6)

Poly(*N*-vinyl-2-pyrrolidone)/KIT-6 (PVP/KIT-6) (0.1 g) and 10 mL of an aqueous acidic solution (C_{HCl} = 0.09 M) of Pd(OAc)₂ (0.025 g, 0.111 mmol) were placed in a round bottom flask. The mixture was heated to 80 °C for 5 h while being stirred under N₂ gas. Then, 0.6 mL (9.71 mmol) aqueous solutions of hydrazine hydrate (N₂H₄·H₂O) (80 vol. %) was added to the mixture drop by drop in 15–20 minutes. After that, the solution was stirred at 60 °C for 1 h. Afterwards, it was filtered and washed sequentially with chloroform and methanol to remove excess N₂H₄·H₂O and was dried at room temperature to yield palladium nanoparticle-poly(*N*-vinyl-2-pyrrolidone)/KIT-6 composite



Scheme 1. Encapsulation of PVP and Pd in the 3D interconnected pore channels of KIT-6.

(Pd-PVP/KIT-6) (Scheme 1). The Pd content of the catalyst was estimated by decomposing the known amount of the catalyst by perchloric acid, nitric acid, fluoric acid, hydrochloric acid, and Pd content was estimated by inductively coupled plasma atomic emission spectrometry (ICP-AES). The Pd content of the catalyst estimated by ICP-AES was 0.98 mmol g^{-1} .

2.4. General procedure for Heck coupling reaction

In the typical procedure for the Heck coupling reaction, a mixture of iodobenzene (1 mmol), styrene (2 mmol), K_2CO_3 (5 mmol), and catalyst (0.14 g, Pd-PVP/KIT-6) in methanol-water (3:1) (5 mL) was placed in a round bottom flask. The suspension was stirred at 60°C for 8 h. The progress of reaction was monitored by Thin Layer Chromatography (TLC) using n-hexane/ethyl acetate (9:1) as eluent. After completion of the reaction (monitored by TLC), for the reaction work-up, the catalyst was removed from the reaction mixture by filtration, and then the reaction product was extracted with CH_2Cl_2 ($3 \times 5 \text{ mL}$). The solvent was removed under reduced pressure. The crude product was purified by flash column chromatography (hexane or hexane/ethyl acetate) to afford the desired coupling product (97% isolated yield). The product was identified with ^1H NMR, ^{13}C NMR and FT-IR spectroscopy techniques.

3. Results and discussion

3.1. Catalyst characterization

The low angle X-ray diffraction patterns of the calcined KIT-6, PVP/KIT-6 and Pd-PVP/KIT-6 are displayed in Fig. 1. The XRD pattern shows a sharp intense peak at $2\theta = 0.95$ corresponding to (211) plane and a hump for (220) and

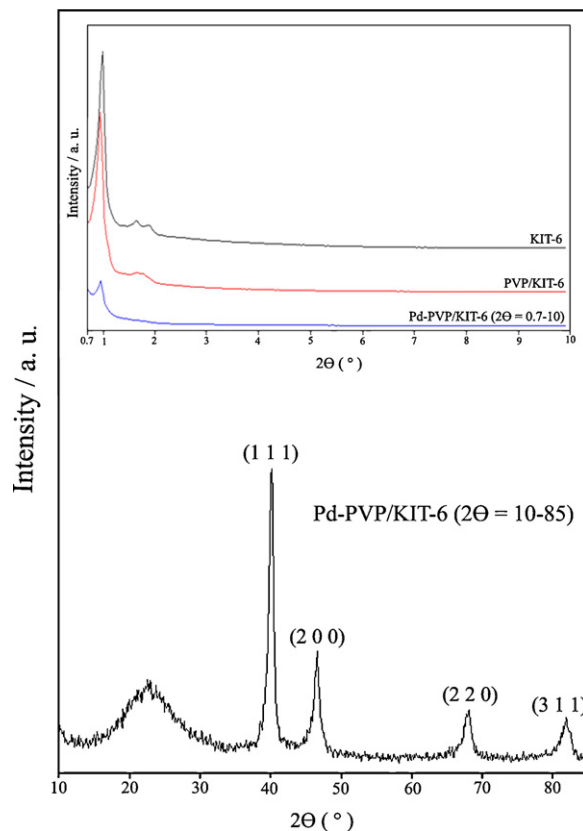


Fig. 1. The powder XRD patterns of mesoporous silica KIT-6, PVP/KIT-6 and Pd-PVP/KIT-6.

Table 1Physicochemical properties of mesoporous silica KIT-6, PVP/KIT-6 and Pd-PVP/KIT-6 samples obtained from XRD and N₂ adsorption.

Sample	BET surface area (m ² g ⁻¹)	V _p (cm ³ g ⁻¹) ^a	BJH pore diameter (nm)	d ₂₁₁ (nm)	a ₀ (nm) ^b
Mesoporous silica KIT-6	989	1.35	4.03	9.23	22.6
PVP/KIT-6	794	1.17	3.53	9.11	22.31
Pd-PVP/KIT-6	500	1.32	4.61	9.5	23.27

^a Total pore volume.^b Unit cell parameter.

(320) planes. The XRD pattern clearly indicates that material is well ordered mesoporous and belongs to bicontinuous cubic space group *la3d* [41]. The PVP/KIT-6 and Pd-PVP/KIT-6 ($2\theta = 0.7$ – 10) samples show the same pattern, indicating that the structure of the KIT-6 (211) is retained even after immobilization with PVP and Pd (Fig. 1). However, the intensity of the characteristic reflection peaks of the PVP/KIT-6 and Pd-PVP/KIT-6 ($2\theta = 0.7$ – 10) samples is found to be reduced (Fig. 1). This may be attributed to the symmetry destroyed by the hybridization of KIT-6 which is also found in the ordered mesoporous silica loading with guest matter [26]. In addition, composites contain much less KIT-6 due to the dilution of the silicious material by PVP and Pd; therefore, this dilution can also account for a decrease in the peak intensity.

The unit cell parameter a_0 of calcined sample calculated from $a_0 = 6^{1/2} d_{211}$ is 22.6 nm, which is in good agreement with the literature and suggests that mesoporous silica is KIT-6 with body centered cubic symmetry (Table 1) [42]. Compared to the d -spacing (or the pore center distance a_0) of KIT-6 and PVP/KIT-6, the incorporation of the Pd nanoparticles into the PVP/KIT-6 pores leads to the expansion of the KIT-6 pore array (Table 1). These results are in good agreement with that obtained from BET observations.

Fig. 1 also shows the wide-angle XRD pattern of the Pd-PVP/KIT-6 nanocomposite ($2\theta = 10$ – 85) (Fig. 1). Four diffraction peaks in the XRD pattern at 39.92° , 46.54° , 67.90° and 81.84° , are the (111), (200), (220) and (311) diffractions of the Pd *fcc* lattice, respectively [43].

Fig. 2 shows the FTIR spectra of KIT-6 (a), PVP/KIT-6 (b), and Pd-PVP/KIT-6 (c). The characteristic bands at around 1080, 815 and 470 cm⁻¹ may be assigned to Si–O–Si asymmetrical stretching vibration, symmetrical stretching vibration and bending vibration, respectively, which is seen in the Fig. 1a,b,c. In addition, the band at around 950–965 cm⁻¹ is related to Si–OH vibrations of the surface silanols (Fig. 2), which is characteristic of mesoporous silica. The existence of PVP in the PVP/KIT-6 composite is evidenced by the appearance of typical PVP vibration on the FTIR spectrum (Fig. 2b). In the FT-IR spectrum of PVP/KIT-6 (Fig. 2b), the new band at 1662 cm⁻¹ is corresponds to the carbonyl bond of PVP [44]. Moreover, the presence of peaks at around 2800–3000 cm⁻¹ corresponds to the aliphatic C–H stretching in PVP/KIT-6 (Fig. 2b). The appearance of the above bands showed that PVP has been attached to the surface of KIT-6 and the PVP/KIT-6 has been obtained. As shown in Pd-PVP/KIT-6 spectrum (Fig. 2c), the band around 1662 cm⁻¹ which corresponds to carbonyl

bond of PVP, is shifted to lower wave numbers (1639 cm⁻¹) (red shift). Moreover, the peak intensity of the carbonyl bond in the spectrum of Pd-PVP/KIT-6 is lower than that of PVP/KIT-6. This may be due to the interaction between the Pd nanoparticles and C=O groups. This means that the double bond CO stretches become weak by coordinating to Pd nanoparticles. Thus, it is confirmed that PVP molecules exist on the surface of the Pd nanoparticles, and coordinate to the Pd nanoparticles [44–46].

N₂ adsorption–desorption isotherms of the KIT-6, PVP/KIT-6 and Pd-PVP/KIT-6 are shown in Fig. 3. The corresponding pore size distribution curves are plotted in Fig. 4. All samples show isotherms of type IV with a sharp capillary condensation step at high relative pressures and H1 hysteric loop, indicative of large channel-like mesopores with a narrow pore size distribution [41]. The BET surface areas, the BJH pore diameters, and the pore volumes for the KIT-6, PVP/KIT-6 and Pd-PVP/KIT-6 nanocomposite are summarized in Table 1. A specific surface area of 989 m² g⁻¹, a large pore volume of

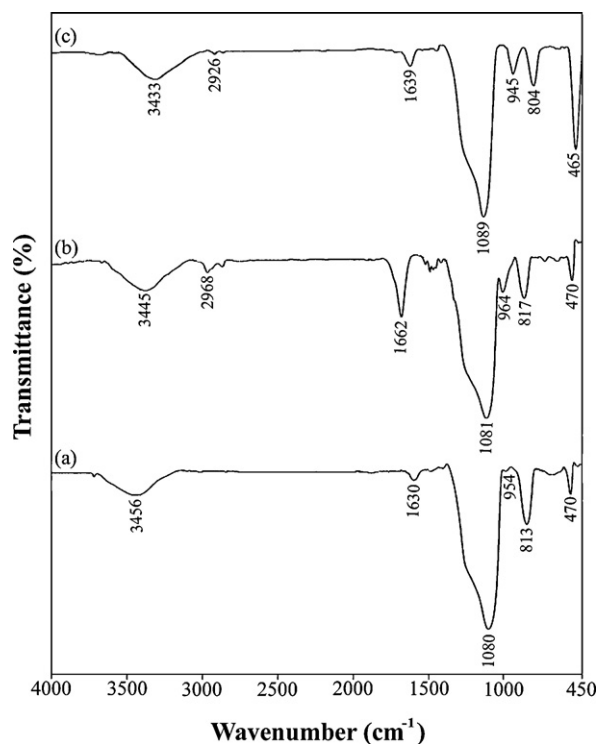


Fig. 2. FT-IR spectra of (a) mesoporous silica KIT-6, (b) PVP/KIT-6 and (c) Pd-PVP/KIT-6.

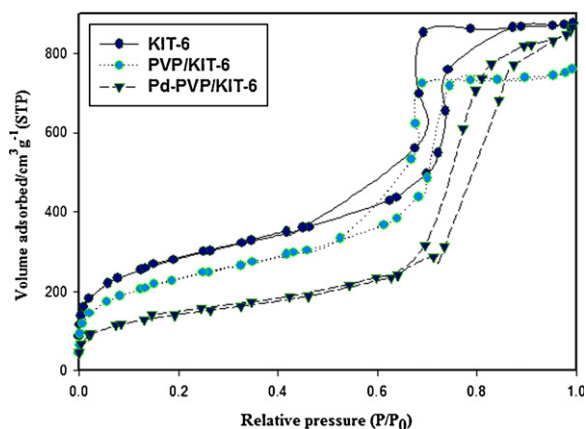


Fig. 3. N_2 adsorption-desorption isotherms of mesoporous silica KIT-6, PVP/KIT-6 and Pd-PVP/KIT-6.

$1.35 \text{ cm}^3 \text{ g}^{-1}$, and a pore size of 4.03 nm are obtained from the isotherm of KIT-6, indicative of its potential application as a host in organic materials. After hybridization with PVP through in situ polymerization, PVP/KIT-6 exhibits a smaller specific area, pore size and pore volume in comparison with those of pure KIT-6, which might be due to the presence of polymer on the surface of the SBA-15 (Table 1 and Fig. 4). However, there is a noticeable increase in pore diameter for Pd-PVP/KIT-6, and the pore volume of Pd-PVP/KIT-6 is a little larger than that of PVP/KIT-6. It might be due to the incorporation of Pd nanoparticles into PVP/KIT-6 [47,48].

According to the results, Pd-PVP/KIT-6 still has a mesoporous form with reasonable surface area ($500 \text{ m}^2 \text{ g}^{-1}$) and it is suitable to act as a catalyst.

Fig. 5 presents the TGA curves of KIT-6 (a), PVP (b), PVP/KIT-6 (c) and Pd-PVP/KIT-6 (d) under N_2 atmosphere. The mass loss at temperatures less than 100°C (around 6%, w/w) is attributed to desorption of water present in the surfaces of the KIT-6 (Fig. 5a). The TGA curves of PVP show a small mass loss (around 7.5%, w/w) in the temperature range $50\text{--}150^\circ\text{C}$, which is apparently associated with adsorbed water (Fig. 5b). At temperatures above 200°C ,

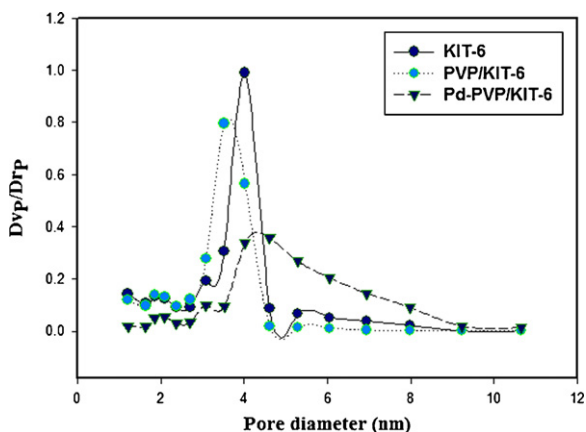


Fig. 4. Pore sizes distribution of KIT-6, PVP/KIT-6 and Pd-PVP/KIT-6. The pore sizes were analyzed with the adsorption branch using the BJH algorithm.

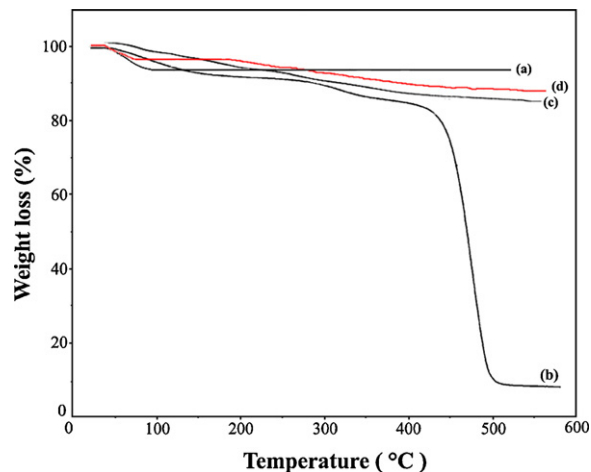


Fig. 5. TGA curves of (a) mesoporous silica KIT-6, (b) PVP, (c) PVP/KIT-6 and (d) Pd-PVP/KIT-6.

PVP shows one main stage of degradation. The mass loss for PVP in the second step is equal to 80% (w/w) which corresponds to the effective degradation of the polymer (Fig. 5b). Thermo analysis of PVP/KIT-6 shows two steps of mass loss (Fig. 5c). The first step (around 3%, w/w) that occurs at temperatures less than 150°C is related to desorption of water. The second step (around 9%, w/w) which appeared at 220°C is attributed to degradation of the polymer, and the degradation ended at 400°C (Fig. 5c). By comparing the PVP and PVP/KIT-6 curves, one can find that PVP/KIT-6 has higher thermal stability and slower degradation rate than PVP (Fig. 5b,c). Therefore, after hybridization, the thermal stability is enhanced and this is very important for the catalyst application. However, for Pd-PVP/KIT-6 sample, two separate weight loss steps are seen (Fig. 5d). The first step (around 5%, w/w) appearing at temperature less than 100°C corresponds to the loss of water. The second weight loss (about $200\text{--}500^\circ\text{C}$) amounts around 6% (w/w) is related to the degradation of the polymer. Obviously, the hybrid Pd-PVP/KIT-6 shows higher thermal stability than PVP/KIT-6. It may be attributed to the presence of Pd nanoparticles in the composite structure. Therefore, it is very important for the catalyst application that the thermal stability was enhanced greatly after hybridization.

Fig. 6 showed the result of UV-Vis spectra of Pd(0)-PVP/KIT-6. According to the literature results, the UV-vis

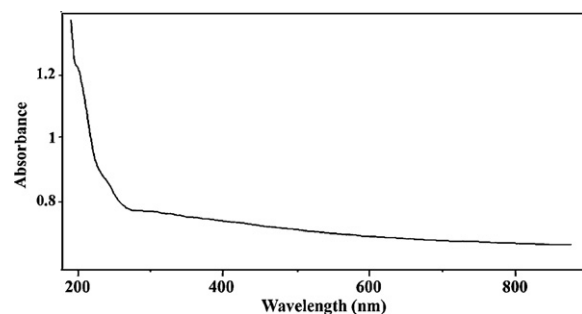


Fig. 6. UV-VIS spectrum of Pd-PVP/KIT-6.

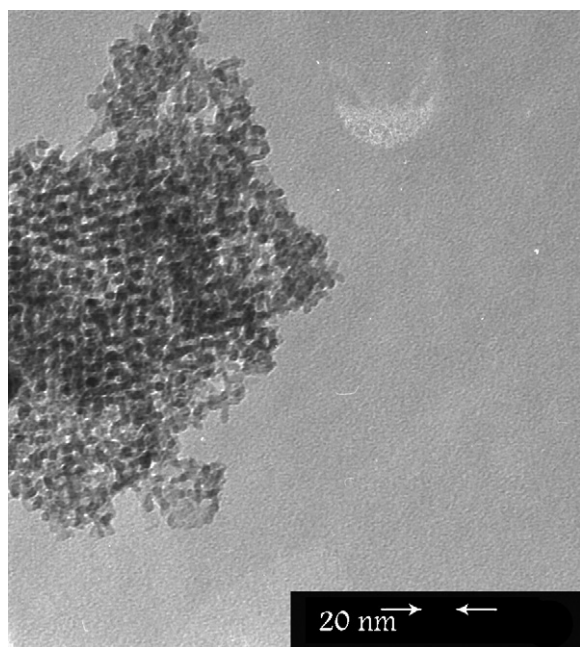


Fig. 7. TEM image for Pd-PVP/KIT-6.

spectra of $\text{Pd}(\text{OAc})_2$ reveal a peak at 400 nm refer to the existence of $\text{Pd}(\text{II})$ [49]. However, as it can be seen from Fig. 6, there is not any peak at 400 nm in the UV-Vis spectra of Pd-PVP/KIT-6, which indicates complete reduction of $\text{Pd}(\text{II})$ to Pd nanoparticles.

The TEM investigations provide the structure of the Pd-PVP/KIT-6 nanocomposite and the distribution of the Pd nanoparticles in the nanocomposite (Fig. 7). The image shows that the ordered cubic $la3d$ mesostructure of KIT-6 is retained and no damage of the periodic structure of the silicate framework is observed. The small dark spots in the images could be ascribed to Pd nanoparticles, located into the support channels (average diameter of ~ 4.5 nm) (Fig. 7). This assumption was confirmed by EDX data, in which the estimated Pd/Si ratio was about 0.1 and it correlated with the loaded Pd amount.

3.2. Catalytic activity

Pd-PVP/KIT-6 nanocomposite was used as a catalyst for Heck reactions of various aryl halides with styrene. To optimize the reaction conditions, a model reaction was carried out by taking iodobenzene and styrene in different solvents and bases at 60°C .

The influence of the solvent on catalytic activity was studied in the coupling of iodobenzene and styrene using Pd-PVP/KIT-6 catalyst and K_2CO_3 as base, at 60°C . The results are summarized in Table 2. When the reactions were conducted in polar solvents, good yield of the product was obtained. The result obtained in the less polar solvent (CH_3CN) were not satisfactory. Among all the solvents, $\text{MeOH}/\text{H}_2\text{O}$ (3:1, v/v) and DMF were the best solvents for this reaction. However, DMF is toxic and has high boiling point, which make it difficult to remove after the reaction. Hence, $\text{MeOH}/\text{H}_2\text{O}$ (3:1, v/v) was finally selected as the

Table 2

Effect of solvent on Heck coupling reaction.^{a,b}

Solvent	Yield (%) ^c
MeOH	90
EtOH	90
DMF	95
CH_3CN	50
H_2O	90
$\text{MeOH}/\text{H}_2\text{O}$ (3:1, v/v)	97

^a Reaction conditions: Pd-PVP/KIT-6 (0.14 g), iodobenzene (1 mmol), styrene (2 mmol), K_2CO_3 (5 eq), solvent (5 mL), 60°C , 8 h.

^b (*E*)/(*Z*) stereo selectivity was higher than 99:1.

^c Isolated yield related to *E* isomer.

solvent for the reaction because it is highly efficient, less expensive, and readily available.

A careful selection of the base in terms of its solubility and basicity in the reaction mixture is extremely crucial. The role of the base in the mechanistic cycle is to re-activate the Pd species in solution, making it available to be recycled back into the reaction mixture [50]. The results revealed that the inorganic bases used were more effective than Et_3N (Table 3), most probably for their complete solubility in $\text{MeOH}/\text{H}_2\text{O}$ (3:1, v/v). Hence, the economically cheaper K_2CO_3 was chosen as base for the coupling reactions. From the data obtained, it can be concluded that the nature of the base plays a significant role in the conversion using Pd nanoparticle-PVP/KIT-6 as catalyst. These observations agree with a previous report in the literature [8].

After the initial optimization studies with iodobenzene and styrene, we conducted the reactions of a variety of aryl halides with styrene with 0.14 g of Pd-PVP/KIT-6 as catalyst. Reactions were carried out in $\text{MeOH}/\text{H}_2\text{O}$ (3:1, v/v) at 60°C at different times. The results are listed in Table 4. In some cases, coupling reactions (entries 2,5,6) required higher time in order to obtain excellent yields. It is well known that activation of C–Cl and C–Br bonds are more difficult than C–I bond, and in general requires harsher reaction conditions in heterogeneous catalysis system. However, chlorobenzene and bromobenzene afforded the expected coupling products in good yield (entries 5,6) but needed more time than that of iodobenzene. Thus, the catalyst afforded excellent yields of the stillbene products at 60°C .

Reusability of the catalyst was tested by carrying out repeated runs of the reaction on the same batch of the catalyst in the case of the model reaction (Table 5). After each cycle, the catalyst was filtered off, washed with water

Table 3

Effect of different bases on Heck reaction.^{a,b}

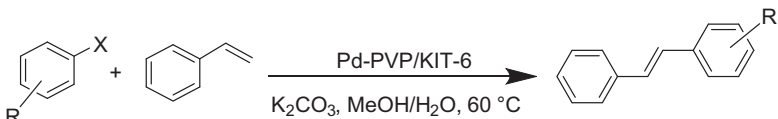
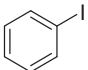
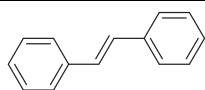
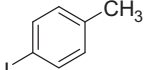
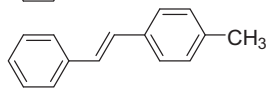
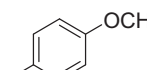
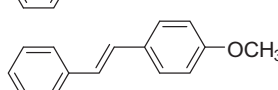
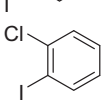
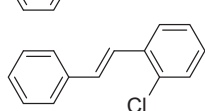
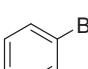
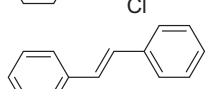
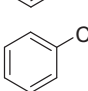
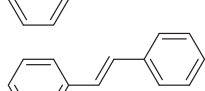
Base	Yield (%) ^c
K_2CO_3	97
Na_3PO_4	74
Et_3N	31

^a Reaction conditions: Pd-PVP/KIT-6 (0.14 g), iodobenzene (1 mmol), styrene (2 mmol), K_2CO_3 (5 eq), $\text{MeOH}/\text{H}_2\text{O}$ (3:1, v/v) (5 mL), 60°C , 8 h.

^b (*E*)/(*Z*) stereo selectivity was higher than 99:1.

^c Isolated yield related to *E* isomer.

Table 4Heck reaction of aromatic aryl halides and styrene catalyzed by Pd-PVP/KIT-6.^{a,b}

						
Entry	Substrate	Product	Yield (%) ^c	Time (h)	Mp (°C)	
					Found	Reported [ref]
1			97	8	122–124	121–123 [51]
2			98	12	117–119	116–118 [51]
3			40	12	136–138	135–137 [51]
4			98	3	38–40	39–40 [52]
5			98	12	122–124	121–123 [51]
6			90	12	122–124	121–123 [51]

^a Reaction conditions: Pd-PVP/KIT-6 (0.14 g), iodobenzene (1 mmol), styrene (2 mmol), K₂CO₃ (5 eq), MeOH/H₂O (3:1, v/v) (5 mL), 60 °C.^b (*E*)/(*Z*) stereo selectivity was higher than 99:1.^c Isolated yield related to *E* isomer.

(10 mL), diethyl ether and acetone (3 × 5 mL). Then, it was dried in oven at 60 °C and reused in the Heck coupling reaction. The results showed that this catalyst could be reused without any modification, eight times and no significant loss of activity/selectivity performance was observed. It should be mentioned that there was very low Pd leaching during the reaction and the catalyst exhibits high stability even after eight recycles (Table 5). Compared

Table 5The catalyst reusability for the Heck reaction.^{a,b}

Cycle	Yield (%) ^c	Pd content of catalyst (mmol/0.14 g)
Fresh	97	0.1372
1	97	0.1372
2	97	0.1372
3	97	0.1372
4	97	0.1370
5	96	0.1369
6	96	0.1369
7	94	0.1365
8	94	0.1365

^a Reaction conditions: Pd-PVP/KIT-6 (0.14 g), iodobenzene (1 mmol), styrene (2 mmol), K₂CO₃ (5 eq), MeOH/H₂O (3:1, v/v) (5 mL), 60 °C, 8 h.^b (*E*)/(*Z*) stereo selectivity was higher than 99:1.^c Isolated yield related to *E* isomer.

to our previous works on composites, using SBA-15 [36–39], Pd-PVP/KIT-6 showed more recyclability. This can be related to the interconnected large-pore cubic mesoporous KIT-6 with three-dimensional (3D) porous networks in comparison to SBA-15 with a two-dimensional (2D) array of pores because three-dimensional porous network of KIT-6 allows for a faster diffusion of reactants, avoids pore blockage, provides more adsorption sites and can prevent leaching of PVP and Pd nanoparticles. The amount of Pd leached was determined by ICP-AES technique (Table 5). The Pd content of the used catalyst (after eight cycles) determined by ICP-AES is 0.975 mmol g^{−1} (0.1365 mmol in 0.14 g catalyst) which is about 0.5% lower than the fresh catalyst (Table 5).

4. Conclusion

A novel polymer–inorganic hybrid material, Pd nanoparticle-PVP/KIT-6, was prepared by a simple and inexpensive method without using any expensive organosilane or bridged organosilanes compound (the organosilica precursors either involve complicated synthesis and purification method or are very expensive). The Pd nanoparticle-PVP/KIT-6 catalyst exhibited a high activity towards the Heck reaction of aryl chlorides, bromides and

iodides at 60 °C without use of toxic ligands or activation. This new heterogeneous catalyst can practically replace soluble catalyst. The catalyst could be easily recycled to eight times without significant loss in reactivity, which are of great importance to the practical applications. Finally, the merit of this methodology was that it was simple, mild, and efficient. Therefore it is believe that the synthetic method reported here would greatly contribute to the environmentally greener and safer process.

Acknowledgements

Support by the Islamic Azad University, Shahreza Branch (IAUSH) Research Council and Center of Excellence in Chemistry is gratefully acknowledged.

References

- [1] A. Balanta, C. Godard, C. Claver, *Chem. Soc. Rev.* 40 (2011) 4973.
- [2] L. Yin, J. Liebscher, *Chem. Rev.* 107 (2007) 133.
- [3] J. Tsuji, *Palladium Reagents and Catalysts-Innovations in Organic Synthesis*, Von Wiley, Chichester, 1995.
- [4] N.J. Whitcombe, K.K. Hii, S.E. Gibson, *Tetrahedron* 57 (2001) 7449.
- [5] V. Polshettiwar, C. Len, A. Fihri, *Coord. Chem. Rev.* 253 (2009) 2599.
- [6] I.P. Beletskaya, A.V. Cheprakov, *Chem. Rev.* 100 (2000) 3009.
- [7] M. Oestreich (Ed.), *The Mizoroki–Heck Reaction*, Wiley, Hoboken, 2009.
- [8] D. Sawant, Y. Wagh, K. Bhatte, A. Panda, B. Bhanage, *Tetrahedron Lett.* 52 (2011) 2390.
- [9] Y. Cui, L. Zhang, *J. Mol. Catal. A: Chem.* 237 (2005) 120.
- [10] M. Shi, H. Qian, *Tetrahedron* 61 (2005) 4949.
- [11] D.Z. Yuan, Q.Y. Zhang, J.B. Dou, *Chin. Chem. Lett.* 21 (2010) 1062.
- [12] F. Berthiol, H. Doucet, M. Santelli, *Tetrahedron Lett.* 45 (2004) 5633.
- [13] S.S. Prockl, W. Kleist, K. Kohler, *Tetrahedron* 61 (2005) 9855.
- [14] A. Corma, H. Garcia, A. Leyva, A. Primo, *Appl. Catal. A: Gen.* 247 (2003) 41.
- [15] R.A. Sanchez-Delgado, N. Machalaba, N. Ng-a-Qui, *Catal. Commun.* 8 (2007) 2115.
- [16] Y. Luo, X. Sun, *Mater. Lett.* 61 (2007) 2015.
- [17] J.M. Thomas, B.F.G. Johnson, R. Raja, G. Sankar, P.A. Midgley, *Acc. Chem. Res.* 36 (2003) 20.
- [18] C.L. Chen, C.Y. Mou, *Nanotechnol. Catal.* 1 (2004) 313.
- [19] D.D. Das, P.J.E. Harlick, A. Sayari, *Catal. Commun.* 8 (2007) 829.
- [20] M. Selvaraj, A. Pandurangan, K.S. Seshadri, P.K. Sinha, K.B. Lal, *Appl. Catal. A: Gen.* 242 (2003) 347.
- [21] R.A. Garcia, R.V. Grieken, J. Iglesias, V. Morales, N. Villajos, *J. Catal.* 274 (2010) 221.
- [22] Y. Park, T. Kang, P. Kimb, J. Yi, *J. Colloid Interface Sci.* 295 (2006) 464.
- [23] F. Kleitz, S.H. Choi, R. Ryoo, *Chem. Commun.* (2003) 2136.
- [24] T.W. Kim, F. Kleitz, B. Paul, R. Ryoo, *J. Am. Chem. Soc.* 127 (2005) 7601.
- [25] F.L. Zhang, Y.H. Zheng, Y.N. Cao, C.Q. Chen, Y.Y. Zhan, X.Y. Lin, Q. Zheng, K.M. Wei, J.F. Zhu, *J. Mater. Chem.* 19 (2009) 2771.
- [26] T. Tsoncheva, L. Ivanova, J. Rosenholm, M. Linden, *Appl. Catal. B Environ.* 89 (2009) 365.
- [27] K. Soni, B.S. Rana, A.K. Sinha, A. Bhaumik, M. Nandi, M. Kumar, G.M. Dhar, *Appl. Catal. B* 90 (2009) 55.
- [28] J.E. Mark, *Acc. Chem. Res.* 39 (2006) 881.
- [29] J. Zheng, G. Li, X. Ma, Y. Wang, G. Wu, Y. Cheng, *Sens. Actuators B* 133 (2008) 374.
- [30] C.M. Chung, S.J. Lee, J.G. Kim, D.O. Jang, *J. Non-Cryst. Solids* 311 (2002) 195.
- [31] N. Ostapenko, G. Dovbeshko, N. Kozlova, S. Suto, A. Watanabe, *Thin Solid Films* 516 (2008) 8944.
- [32] G. Morales, R. van Grieken, A. Martin, F. Martinez, *Chem. Eng. J.* 161 (2010) 388.
- [33] B. Gao, D. Kong, Y. Zhang, *J. Mol. Catal. A: Chem.* 286 (2008) 143.
- [34] Z.H. Ma, H.B. Han, Z.B. Zhou, J. Nie, *J. Mol. Catal. A: Chem.* 311 (2009) 46.
- [35] M.H. Alves, A. Riondel, J.M. Paul, M. Birot, H. Deleuze, *C. R. Chimie* 13 (2010) 1301.
- [36] R.J. Kalbasi, M. Kolahdoozan, A.R. Massah, K. Shahabian, *Bull. Korean Chem. Soc.* 31 (2010) 2618.
- [37] R.J. Kalbasi, M. Kolahdoozan, M. Rezaei, *Mater. Chem. Phys.* 125 (2011) 784.
- [38] R.J. Kalbasi, A.A. Nourbakhsh, F. Babaknezhad, *Catal. Commun.* 12 (2011) 955.
- [39] R.J. Kalbasi, M. Kolahdoozan, K. Shahabian, F. Zamani, *Catal. Commun.* 11 (2010) 1109.
- [40] M.T. Run, S.Z. Wu, D.Y. Zhang, G. Wu, *Mater. Chem. Phys.* 105 (2007) 341.
- [41] Y. Teng, X. Wu, Q. Zhou, C. Chena, H. Zhao, M. Lan, *Sens. Actuators B* 142 (2009) 267.
- [42] D. Zhang, A. Duan, Z. Zhao, C. Xu, *J. Catal.* 274 (2010) 273.
- [43] P. Wang, Z. Wang, J. Li, Y. Bai, *Micropor. Mesopor. Mater.* 116 (2008) 400.
- [44] T. Iwamoto, K. Matsumoto, T. Matsushita, M. Inokuchi, N. Toshima, *J. Colloid Interface Sci.* 336 (2009) 879.
- [45] O. Metin, S. Ozkar, *J. Mol. Catal. A: Chem.* 295 (2008) 39.
- [46] H. Hirai, H. Chawanya, N. Toshima, *React. Polym.* 3 (1985) 127.
- [47] H. Song, R.M. Rioux, J.D. Hoefelmeyer, R. Komor, K. Niesz, M. Grass, P. Yang, G.A. Somorjai, *J. Am. Chem. Soc.* 128 (2006) 3027.
- [48] S. Chytil, W.R. Glomm, E. Vollebakk, H. Bergem, J. Walmsley, J. Sjoblom, E.A. Blekkan, *Micropor. Mesopor. Mater.* 86 (2005) 198.
- [49] P. Ahmadian Namini, A.A. Babaluo, B. Bayati, *Int. J. Nanosci. Nanotech.* 3 (2007) 37.
- [50] G.T. Crisp, *Chem. Soc. Rev.* 27 (1998) 427.
- [51] N. Iranpoor, H. Firouzabadi, A. Tarassoli, M. Fereidoonhezad, *Tetrahedron* 66 (2010) 2415.
- [52] Y. Leng, F. Yang, K. Wei, Y. Wu, *Tetrahedron* 66 (2010) 1244.